Applied Physics Letters

Nanoscale x-ray magnetic circular dichroism probing of electric-field-induced magnetic switching in multiferroic nanostructures

Cite as: Appl. Phys. Lett. **90**, 123104 (2007); https://doi.org/10.1063/1.2714201
Submitted: 20 December 2006 . Accepted: 09 February 2007 . Published Online: 20 March 2007

T. Zhao, A. Scholl, F. Zavaliche, H. Zheng, M. Barry, A. Doran, K. Lee, M. P. Cruz, and R. Ramesh

Nanoscale x-ray magnetic circular dichroism probing of electric-field-induced magnetic switching in multiferroic nanostructures

T. Zhao[a)]
Department of Physics, University of California, Berkeley, California 94720 and Department of Materials Science and Engineering, University of California, Berkeley, California 94720

A. Scholl
Advanced Light Source, Lawrence Berkeley National Laboratory, Berkeley, California 94720

F. Zavaliche, H. Zheng, and M. Barry
Department of Physics, University of California, Berkeley, California 94720 and Department of Materials Science and Engineering, University of California, Berkeley, California 94720

A. Doran
Advanced Light Source, Lawrence Berkeley National Laboratory, Berkeley, California 94720

K. Lee
Department of Physics, University of California, Berkeley, California 94720 and Department of Materials Science and Engineering, University of California, Berkeley, California 94720

M. P. Cruz
Department of Physics, University of California, Berkeley, California 94720; Department of Materials Science and Engineering, University of California, Berkeley, California 94720; and Centro de Ciencias de la Materia Condensada, Universidad Nacional Autonóma de México, Km 107, Carretera Tijuana-Ensenada, CP 22800 Ensenada, Baja California, Mexico

R. Ramesh[b)]
Department of Physics, University of California, Berkeley, California 94720 and Department of Materials Science and Engineering, University of California, Berkeley, California 94720

(Received 20 December 2006; accepted 9 February 2007; published online 20 March 2007)

The magnetic structure as well as its response to an external electric field were studied in ferrimagnetic $CoFe_2O_4$ nanopillars embedded in an epitaxial ferroelectric $BiFeO_3$ film using photoemission electron microscopy and x-ray magnetic circular dichroism. Magnetic switching was observed in both Co and Fe magnetic sublattices after application of an electric field. About 50% of the $CoFe_2O_4$ nanopillars were measured to switch their magnetization with the electric field, implying an elastic-mediated electric-field-induced magnetic anisotropy change. © *2007 American Institute of Physics*. [DOI: 10.1063/1.2714201]

Multiferroic materials blending magnetic and electric orders have become an exciting research topic in recent years due to the broad range of potential applications and the intriguing science behind the phenomenon.[1–9] In previous works, we demonstrated the epitaxial growth of ferrimagnetic $CoFe_2O_4$ (CFO) nanopillars embedded in a single crystalline ferroelectric $BaTiO_3$ or $BiFeO_3$ (BFO) matrix and observed an electric-field-induced magnetization switching in the BFO-CFO nanostructures.[7–9] However, no quantitative magnetic information could be obtained. Also, the physical mechanism behind the observed magnetic switching by an electric field stayed unclear.[8] Moreover, bulk CFO shows an inverse-spinel structure and the magnetic Co and Fe atoms contribute differently to the ferrimagnetic behavior.[10,11] It is therefore of great interest to study the contribution from each magnetic sublattice separately before and after an electrical poling. In this work, we quantitatively study the magnetic structure of a BFO-CFO nanocomposite by performing x-ray magnetic circular dichroism (XMCD)-based (Refs. 12 and 13) photoemission electron microscopy (PEEM) (Ref. 14) measurements at beamline 7.3.1.1 at the Advanced Light Source.

A 300-nm-thick epitaxial film composed of ferrimagnetic CFO pillars embedded in BFO matrix, with a relative volume ratio of 35/65, was prepared by pulsed laser deposition (PLD) on a (001) oriented $SrTiO_3$ single crystal substrate with a 50-nm-thick conductive epitaxial $SrRuO_3$ layer deposited by PLD as well. Three-dimensional epitaxy as a consequence of complete phase separation was confirmed by x-ray diffraction and transmission electron microscopy.[7–9] Piezoelectric force microscope (PFM), magnetic force microscope (MFM), and superconducting quantum interference device (SQUID) measurements confirmed the coexistence of ferroelectricity and magnetism in the nanostructure. The film was magnetized in an out-of-plane 20 kOe magnetic field, resulting in a predominant downward magnetization confirmed by MFM and SQUID. Then, an electric voltage of −12 V was applied in order to switch the ferroelectric polarization in the BFO matrix by scanning the PFM tip over a selected area ($\sim 8 \times 8\ \mu m^2$). Subsequently, XMCD measurements on individual pillars as well as on larger areas containing many pillars were performed in both poled and unpoled regions.

Figures 1(a) and 1(b) show two absorption spectra acquired in an unpoled area using left and right circularly po-

[a)]Present address: Seagate Research, 1251 Waterfront Place, Pittsburgh, PA 15222; electronic mail: tong.zhao@seagate.com
[b)]Electronic mail: rramesh@berkeley.edu

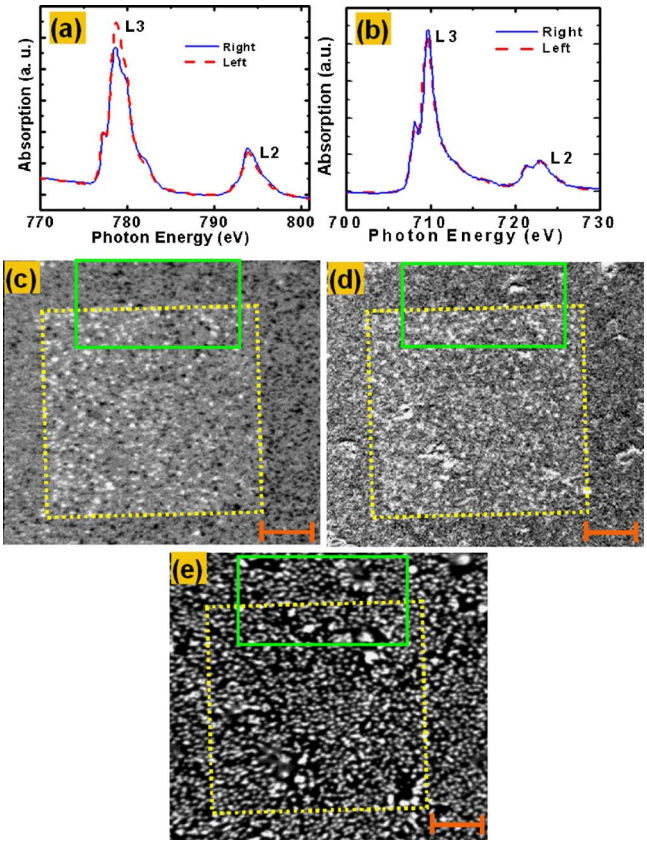

FIG. 1. (Color online) (a) Co-edge and (b) Fe-edge x-ray absorption spectra. (c) Co-edge XMCD, (d) Fe-edge XMCD, and (e) Co element-contrast PEEM images. The scale bars in (c), (d), and (e) are 2 μm.

larized x rays, in the vicinity of the Co L and Fe L edges, respectively (circular polarization ~75%). The difference between the two spectra in each figure is the magnetic dichroism, which is a measure for the magnetic moment of the corresponding species. The dichroism value is maximum at the L_3 and L_2 absorption peaks and changes sign between them.[12] PEEM images were taken at the L_3 energy positions with right and left circular polarizations, respectively. Then, the PEEM data with right circular polarization were divided by the data with left polarization as shown in Figs. 1(c) for the Co edge and 1(d) for the Fe edge. Opposite magnetization states of different pillars lead to opposite dichroisms and thus opposite contrasts (black and white) in the PEEM images; the gray color indicates a nonmagnetic background from the BFO matrix. To ascertain that the dichroism contrast seen in Figs. 1(c) and 1(d) originates from CFO nanopillars, two PEEM images were taken on the left shoulder of the Co L_3 peak with right and left circular polarizations, respectively. Then, the sum of the two images, as shown in Fig. 1(e), contains elemental contrast only. The dashed squares in the PEEM pictures outline an area electrically poled at −12 V. The white areas in Fig. 1(e) indicate the presence of Co (CFO pillars), while the black ones do not contain Co (BFO matrix). By comparing Figs. 1(c)–1(e), areas showing a magnetic contrast in Figs. 1(c) and 1(d) correspond to areas containing Co in Fig. 1(e), i.e., CFO pillars, which can be seen more clearly in Fig. 2. Figures 2(a) and 2(b) are zoomed-in images of Figs. 1(c) and 1(e), respectively, at an area on the poling-nonpoling border outlined by the solid boxes in Figs. 1(c)–1(e). The boxes with solid and dashed lines in Fig. 2 indicate an unpoled and a

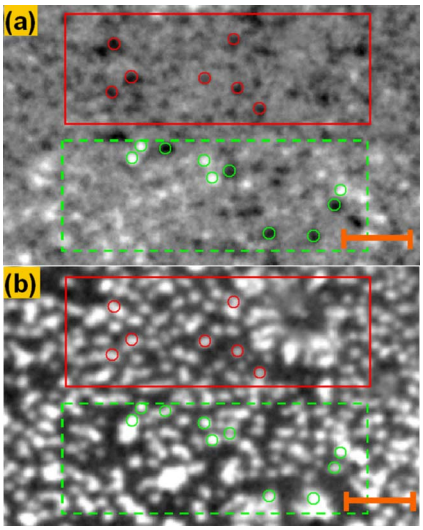

FIG. 2. (Color online) Enlarged Co-edge PEEM images in an area outlined by the solid boxes at the interface between poled and unpoled regions in Figs. 1(c)–1(e). (a) Magnetic information. (b) Chemical information. The scale bars are 1 μm.

poled area, respectively. Individual CFO nanopillars can be seen clearly in all the PEEM images. In the XMCD PEEM images [Figs. 1(c), 1(d), and 2(a)], only black dots can be seen in the unpoled area, indicating a uniform downward magnetization distribution, while both black and white dots can be seen in the poled area, indicating switching of some of the nanopillars.

Figures 3(a) and 3(c) show Co and Fe dichroism spectra, obtained by subtracting absorption spectra acquired using left and right circularly polarized x rays, for seven individual CFO pillars marked by circles in the solid box in Fig. 2(a) in the unpoled area. The spectra were shifted along the y axis for clarity. Figures 3(b) and 3(d) show Co and Fe dichroism spectra, averaged across an unpoled area marked by the solid box in Fig. 2(a). An ~20% dichroism was measured on individual pillars as well as on average over a large area, indicating a saturated Co magnetization in the unpoled CFO pillars. The area averaged dichroism of Fe is smaller than that on individual pillars because the Fe atoms in the BFO matrix contribute to the average absorption spectrum, but not significantly to the total magnetization since BFO is antiferromagnetically ordered.[15] In an ideal inverse-spinel structure, Co^{2+} cations occupy half of the octahedral sites, while Fe^{3+} occupy the other half and all tetrahedral sites. The spin orientation of the Fe^{3+} atoms on the two spinel sites is opposite to each other as indicated by the two dichroism peaks with opposite polarities, labeled as Fe^{3+} Oct. and Fe^{3+} Tetr. in Fig. 3(d). Interestingly, a third peak corresponding to the other half of the octahedral sites (labeled as Fe^{2+} Oct.) is also observed in the Fe dichroism spectra. Therefore, some of the Co^{2+} are replaced by Fe^{2+} at the octahedral sites, as was reported before.[11,16]

Figures 4(a) and 4(b) show the dichroism spectra at the Co edge obtained by the same method as in Fig. 3 on CFO pillars in a poled area labeled by the dashed box in Fig. 2(a). CFO pillars with opposite PEEM contrast were selected as shown in Fig. 2(a). Figure 4(a) shows CFO with contrast opposite to those in the unpoled area, while Fig. 4(b) is for those with the same contrast. It is clear that the dichroism spectra have similar structures before and after the electrical

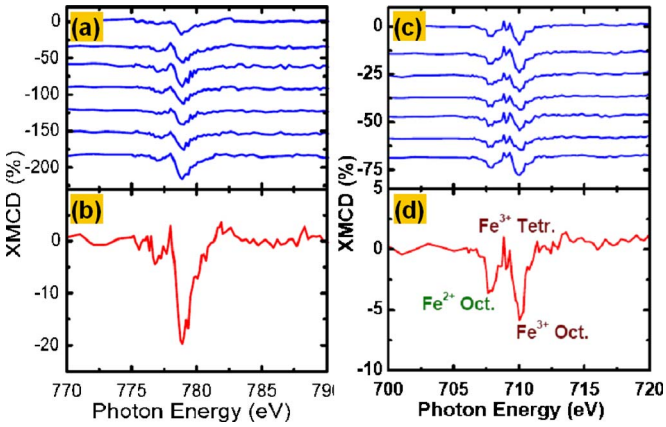

FIG. 3. (Color online) XMCD in an unpoled area as labeled by the solid boxes in Fig. 2 between right and left circularly polarized x rays on [(a) and (b)] Co edge and [(c) and (d)] Fe edge. (a) and (c) are on seven individual CFO pillars marked by circles in the solid boxes in Fig. 2, while (b) and (d) are averaged over the solid box area.

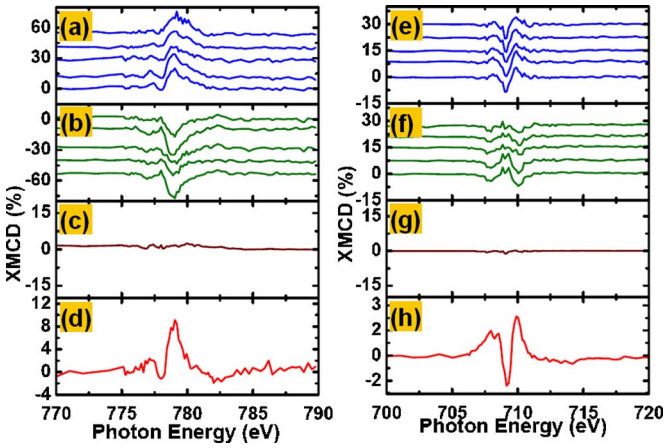

FIG. 4. (Color online) XMCD in a poled area labeled by the dashed boxes in Fig. 2 between left and right polarizations on [(a)–(c)] Co edge and [(e)–(g)] Fe edge. (a), (b), (e), and (f) are on individual pillars with opposite PEEM contrast marked by circles in the dashed boxes in Fig. 2, while (c) and (g) are averaged over the dashed box area. XMCD between a poled region (dashed box) and an unpoled region (solid box) in Fig. 2 on (d) Co edge and (h) Fe edge by using right circularly polarized x ray.

poling, indicating a similar magnetic structure. The magnitude of the dichroism of the switched pillars is the same as that of the pillars that did not switch, indicating complete magnetic switching. Similar results were obtained at the Fe edge, as shown in Figs. 4(e) and 4(f). It is clear that after electrical poling both the Co and the Fe magnetic sublattices switch individually and result in an overall opposite magnetization.

An almost zero average dichroism, thus a zero magnetization, over the poled area marked with the dashed box in Fig. 2(a) was measured at both Co and Fe edges, as shown in Figs. 4(c) and 4(g), respectively, indicating that about 50% of the CFO pillars switched their magnetization. This is further confirmed by the dichroism between the poled and the unpoled areas (dashed and solid boxes in Fig. 2, respectively) at both the Co and Fe edges by using right circularly polarized x ray, as shown in Figs. 4(d) and 4(h). The dichroism peaks reveal a difference in magnetization between the two areas with maximum dichroism values of 10% and 3% at the Co and Fe edges, respectively. These values are half of the dichroism measured on single pillars. This means that the average magnetization difference between the poled and unpoled areas $(\mathbf{M}-0)$ is 50% of the difference between two opposite magnetization directions $[\mathbf{M}-(-\mathbf{M})]$ on a single pillar. XMCD measurements clearly reveal that 50% of the CFO pillars switched their magnetization by an electrical field.

When an electric field is applied on the BFO-CFO nanostructure, elastic strain is generated in the BFO matrix due to the lattice distortion associated with ferroelectric polarization switching and reverse piezoelectric effect. The elastic strain in the BFO matrix transfers into the CFO pillars and changes their magnetic easy axis from out of plane to in plane due to its high magnetostriction. During this process, the magnetic polarization flips to in plane. After the electric field is removed, the magnetization flips back evenly to the two perpendicular directions, and a mixture of 50% up and 50% down in the final magnetic state should be expected. The ability to change the magnetic anisotropy is the critical first step to locally lower the magnetic coercivity, which should be very useful for magnetic recording techniques.

In summary, XMCD-based PEEM measurements were performed on a BFO-CFO nanocomposite. The magnetic structure on individual ferrimagnetic CFO nanopillars was directly measured using x-ray microscopy. The XMCD studies confirm switching of both Co and Fe magnetic sublattices, resulting in a complete reversal of the magnetization of individual CFO pillars by the electric field. Quantitative measurements reveal that 50% of the pillars switch by the electrical poling, which supports the scenario of a strain-induced magnetic anisotropy change and a random magnetic switching through magnetoelectric coupling.

The authors acknowledge support of ONR Grant No. N00014-04-1-0426 and ONR-MURI Grant No. E-21-6RU-G4. Partial support from a LBL LDRD program is also acknowledged. The Advanced Light Source is supported by the U.S. Department of Energy under Contract No. DE-AC02-05CH11231.

[1] W. Eerenstein, N. D. Mathur, and J. F. Scott, Nature (London) **442**, 759 (2006).
[2] Y. Tokura, Science **312**, 1481 (2006).
[3] N. A. Spaldin and M. Fiebig, Science **309**, 391 (2005).
[4] N. A. Hill, J. Phys. Chem. B **104**, 6694 (2000).
[5] S. Shastry, G. Srinivasan, M. I. Bichurin, V. M. Petrov, and A. S. Takarenko, Phys. Rev. B **70**, 064416 (2004).
[6] S. Dong, J. F. Li, and D. Viehland, Philos. Mag. Lett. **83**, 769 (2003).
[7] H. Zheng, J. Wang, S. E. Lofland, Z. Ma, L. Mohaddes-Ardabili, T. Zhao, L. Salamance-Riba, S. R. Shinde, S. B. Ogale, F. Bai, D. Viehland, Y. Jia, D. G. Schlom, M. Wuttig, A. Roytburd, and R. Ramesh, Science **303**, 661 (2004).
[8] F. Zavaliche, H. Zheng, L. Mohaddes-Ardabili, S. Y. Yang, Q. Zhan, P. Shafer, E. Reilly, R. Chopdekar, Y. Jia, P. Wright, D. G. Schlom, Y. Suzuki, and R. Ramesh, Nano Lett. **5**, 1793 (2005).
[9] H. Zheng, Q. Zhan, F. Zavaliche, M. Sherburne, F. Straub, M. P. Cruz, L.-Q. Chen, U. Dahmen, and R. Ramesh, Nano Lett. **6**, 1401 (2006).
[10] R. J. Hill, J. R. Craig, and G. V. Gibbs, Phys. Chem. Miner. **3**, 317 (1979).
[11] R. A. D. Pattrick, G. van der Laan, C. M. B. Henderson, P. Kuiper, E. Dudzik, and D. Vaughan, Eur. J. Mineral. **14**, 1095 (2002).
[12] J. Stohr, Science **259**, 658 (1993).
[13] J. Stohr, H. A. Padmore, S. Anders, T. Stammler, and M. R. Scheinfein, Surf. Rev. Lett. **5**, 1297 (1998).
[14] A. Scholl, H. Ohldag, F. Nolting, J. Stohr, and H. A. Padmore, Rev. Sci. Instrum. **70**, 3973 (1999).
[15] Y. P. Fischer, M. Polomska, I. Sosnowska, and M. Szymanski, J. Phys. C **13**, 1931 (1980).
[16] G. A. Sawatzky, F. van deer Woude, and A. H. Morrish, J. Appl. Phys. **39**, 1204 (1968).